nature climate change

SUPPLEMENTARY INFORMATION

DOI: 10.1038/NCLIMATE2568

Causal feedbacks in climate change

Egbert H. van Nes*, Marten Scheffer, Victor Brovkin, Timothy M. Lenton, Hao Ye, Ethan Deyle, and George Sugihara*

*correspondence to: egbert.vannes@wur.nl and gsugihara@ucsd.edu

This PDF file includes:

- Supplementary Text
- Figs. S1 to S15
- Tables S1 to S3

Supplementary Text

A moving window scan of time lags

We used a simple method to find the optimal displacement for correlation between subsets of two time series. We used moving windows to determine the subsets of both datasets and computed the cross-correlation between windows with positive and negative time displacements. We define the optimum lag as that which yields the maximum Pearson correlation coefficient between the lagged windows. We illustrate this method with two models that have chaotic dynamics in addition to the CO_2 and temperature data of the Vostok data set[1], see Figure S1.

First we generated time series with the famous Lorenz system[31]:

$$\frac{dx}{dt} = \sigma\,(y - x)$$

$$\frac{dy}{dt} = r\,x - x\,z - y$$

$$\frac{dz}{dt} = x\,y - b\,z$$

b = 8/3; r = 28; σ = 10;

Additionally we applied the method to a discrete two species logistic growth model:

$$X_i(t+1) = X_i(t)\left(r_i - \sum_j \alpha_{ij}\,X_j(t)\right)$$

$\alpha_{11} = 3.8$; $\alpha_{12} = 0.02$; $\alpha_{21} = 0.1$; $\alpha_{22} = 3.5$; $r_1 = 3.8$; $r_2 = 3.5$

Sensitivity to the used data set

We tested the robustness of our CCM analysis[8] of greenhouse gasses and temperature[1] by comparing our results with those from other data sets. In particular we tested data obtained from the oldest part of the EPICA ice core data (-800 to -400 kyr) [24,25] and a recent high resolution data set (-22 to 0 kyr), that were constructed from different ice cores[21] (Figure S2). The EPICA ice core data were downloaded from:

- http://www.ncdc.noaa.gov/paleo/metadata/noaa-icecore-6091.html (CO_2)
- http://www.ncdc.noaa.gov/paleo/pubs/loulergue2008/loulergue2008.html (CH_4)
- and the high resolution data set from the supplementary materials of [21].

The latter data set was interpolated on 100 year intervals. All data sets gave similar patterns (Figure S2), although the high-resolution data set failed to be significantly different from the null model. However, this is likely due to the fact that this data set only consisted of 135 highly auto-correlated points, limiting the statistical power of CCM analysis.

Sensitivity to the parameters of CCM, interpolation and significance testing

To apply CCM, we need to choose several parameters, such as the embedding lag τ and the embedding dimension E. In Figure S3 we show that these parameters have little effect on the maximum CCM skill. In addition, the method of interpolation (spline vs. linear interpolation) did not have much effect on the results (Table S1 and S2). Subsetting the original data also had a relatively small effect on the average CCM skill (Fig. S4), although the results were less strong, for obvious reasons. Finally, we employed surrogate time series to quantify significance. We used two conservative null models (phase shifts on Fourier transformed data[30] and random phase shift of the whole data set), which produced similar outcomes (Fig. 2 and Fig. S5). Thus, we conclude that CCM is robust and our results are not sensitive to our choice of embedding parameters or interpolation method.

Results for other climate and orbital variables and effects of filtering

We also analyzed the CCM skill between the main variables analyzed in the text (CO_2 and temperature) and two other climate indicators from the ice-core: dust content (desert aerosols) and sodium content in the ice (marine aerosols) [1]. The CCM skills for both dust and sodium were significantly different from the null model (Fig. S6).

In addition we explored whether orbital forcing would be clearer if we replaced insolation with Fig. S7):

- Eccentricity - eccentricity of the earth's orbit
- Obliquity - axial tilt of the earth
- Precession - change in the orientation of the rotational axis of the earth
- Omega - longitude of perihelion from moving vernal equinox in degrees

None of these orbital parameters resulted in CCM skills significantly different from the null model.

In addition, we tested whether filtering high frequencies out of CO_2 and temperature could improve CCM skills linking climate to orbital forcing. We used Gaussian filtering (ksmooth) with a bandwidth of 6 kyr to create time series containing just low-frequency variability. However there was no improvement in the CCM results (Fig. S8). We

calculated the optimal time displacement of CCM for all pairwise variable combinations (Fig. S9).

Null-models with unidirectional forcing of temperature or CO2

Sugihara et al. [8] warn that CCM may falsely suggest two-way causality if two variables have highly synchronized dynamics. Such strong correlation between variables can occur if one variable has a very strong effect on the other, such that the forced variable is a 'slave' of the forcing variable. Here, we examine two simple dynamical models with strong one-way forcing, to investigate the effects of synchronicity on CCM.

Models:

(1) Dynamical CO_2 forced by Temperature:

We follow the approach of Scheffer et al.[32] to model CO_2 dynamically but forced by temperature:

$$C_0 = \alpha(T - T_0) + C_{ref}$$

$$\frac{dC}{dt} = r_C(C_0 - C) - m_C(t)$$

$m_C(t)$ is a autocorrelated external variable that represents other forcing factors. We used the actual measured temperature proxies to force the CO_2. (r_C is used to tune the relative forcing, all other parameters (α and C_{ref}) are calibrated).

(2) Dynamical temperature forced by CO_2:

We use the following equation to calculate the equilibrium temperature (T_0) based on CO_2 (C) (see [32])

$$T_0 = \frac{s}{ln(2)} \ln\left(\frac{C}{C_{ref}}\right)$$

Temperature is modelled with a stochastically forced model where the model approaches the equilibrium T_0 exponentially with a rate r_T:

$$\frac{dT}{dt} = r_T(T_0 - T) - m_T(t)$$

$m_T(t)$ is an autocorrelated external variable that represents other forcing factors. We used the actual measured CO_2 proxies to force the temperature. (r_T is used to tune the relative forcing, all other parameters (s and C_{ref}) are calibrated).

Analyses:

The high frequencies of the Vostok core data were assumed to represent mainly observational error. To mimic the same amount of observational error for the null models, we added independent and identically distributed observational error to the model results. The magnitude and variance were determined from the distribution of the difference between the interpolated time series and a kernel smoothed time series (6 kyr Gaussian filter) of temperature and CO_2 from the Vostok data[1]. The models were forced by either the interpolated CO_2 or temperature time series from the Vostok ice core data[1]. The parameters of the model and the amount of noise of the autocorrelated external variables (m_C(t) and m_T(t)) we added was fitted such that the generated time series resembled the Vostok ice core data.

With both models we generated time series and computed the CCM skill of the forced variable with respect to the forcing variable and vice versa. We tested 10 surrogate time series for each value of the r_T and r_C parameters (speed of convergence), as this parameter had a clear effect on the results (Fig. S11). We followed the same procedures as for the actual data (E =4, τ = 2 kyr, and 500 bootstrapped library sets of length 100). For each resampled library, we determined the optimal time displacement of the cross mapped variable (i.e. how much to adjust the "causal" variable forward or backward in time). The optimum displacements for the simulated data turned out to be asymmetrical; the optimum time displacement for the effect of temperature on CO_2 was more negative than that for the opposite direction. We tested statistically whether this asymmetry in CO_2 and temperature was different for the Vostok data set compared to both null models using a randomization test.

Results

Our results confirm that CCM may suggest two-way causality if one of the variables is merely a "slave" of the other (i.e. there is a strong one way causal effect) (Fig. S10). In fact, for our null models, the CCM measure of the influence of the slaved variable on the forcing variable is generally stronger, despite the lack of causation in this direction. Thus, if we consider only the direct observed cross mapping results we cannot distinguish bidirectional forcing from strong one-way forcing between temperature and CO_2 in the actual data.

Consequently, we take an additional step and analyze the optimal time displacement between both time-series for cross mapping (Fig. S11). We expect that for a real causal effect, the optimal displacement will be negative for cross mapping, such that the forced variable is better at estimating the past values of the causal variable that influenced it, rather than present or future values, which have not had an effect yet. For synchronous time series, we expect the optimal lag to be around -2 kyr given the embedding dimension E = 4 and embedding lag τ = 2, because the optimal lag should fall within the range of time lags of the vector being used for cross-mapping. For example, with embedding dimension E = 4, and embedding lag τ = 2, the vectors will have the form $\langle X(t), X(t-2), X(t-4), X(t-6)\rangle$ and are used to cross-map $Y(t+t_p)$. For correlated series, we expect the optimal lag (t_p) to lie in the middle of the range, as the symmetry of forward and backward lags gives the best estimate of the system state (see also Fig. S12), though this precise symmetry is not a general phenomenon.

Fig. S11 shows that a negative optimal lag exceeding the null expectation occurs if the speed of processes is slow enough. Thus, CCM at an optimal lag beyond that of the null model must necessarily imply true causality. Note that this is fundamentally different from merely detecting lagged correlation between time-series; CCM measures how well a variable can be predicted from the history of another variable, rather than the simple linear measure of correlation.

The sensitivity of these results can be quantified by computing how a systematic misalignment error in the CO_2 and temperature time series affects the finding that there is a significant causal lag of CO_2 behind temperature. We define an alignment error of x years to mean that the temperature time series is dated x years older than it actually is (i.e. temperature needs to be shifted forward x years to be correct). Note that this

alignment error means that the corrected optimal lag in the temperature *xmap* CO_2 direction will be smaller by x, and that the corrected optimal lag in the opposite direction will be larger by x. In other words, the difference in optimal lags will actually change by 2x.

As long as >95% of the bootstrap samples show a positive difference in the optimal lag (i.e. that temperature precedes CO_2), there is significant evidence that temperature has a causal effect on CO_2. Figure S13 plots alignment error (kyr) vs. the p-value for this test (that temperature precedes CO_2). The intersection of the blue dashed line ($p = 0.05$) with the realized empirical CDF indicates that a misalignment of up to ~1160 years can occur that will not affect the significance of our results.

References (see also main text)

31 Lorenz, E. N. Deterministic nonperiodic flow. *Journal of Atmospheric Sciences* **20**, 130-141 (1963).

32 Scheffer, M., Brovkin, V. & Cox, P. M. Positive feedback between global warming and atmospheric CO_2 concentration inferred from past climate change. *Geophys. Res. Lett.* **33**, L10702 (2006).

Supplementary Figures

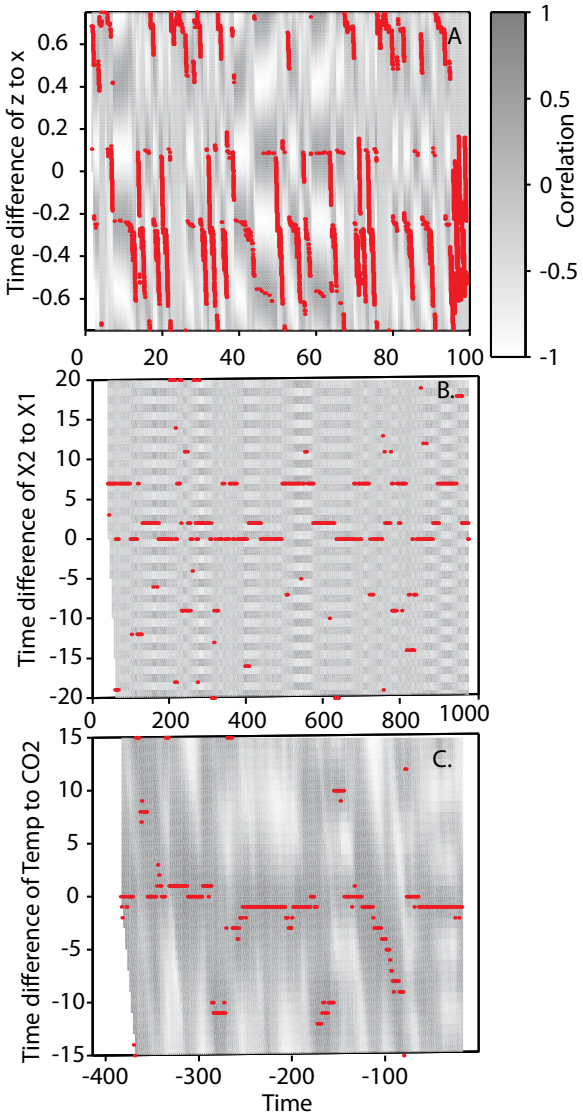

Fig. S1.

The time displacement giving optimum correlation within sliding windows. The correlation is displayed as a greyscale. Red dots indicate the time differences with the maximum correlation (negative=lag, positive=lead). A. Simulated data (x and z) from the coupled Lorenz system[31], sliding window=1.5 time units (resolution 0.05 time units). B. Simulated data from the coupled two-species logistic competition model, sliding window = 41 time steps. C. Linearly interpolated temperature and CO_2 from the Vostok ice core data[1], sliding window = 31 kyr (resolution 1 kyr).

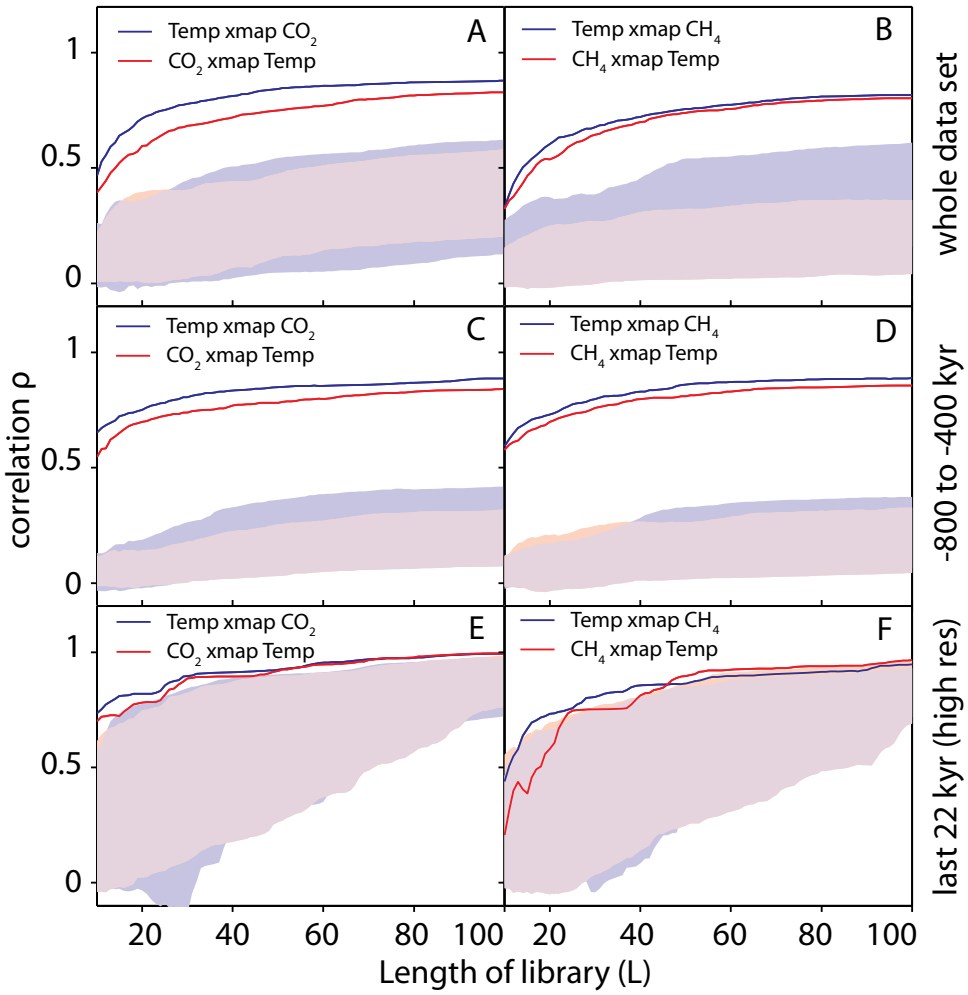

Fig. S2.

Correlation of cross mapped versus observed values as a function of the length of the time series. Shaded areas are the 5th to 95th percentiles of CCM skill for 100 surrogate time series from the null model (swap model; see Methods. CCM is shown for A,B the combined EPICA and Vostok cores (-798 kyr BP to present); C,D the oldest part of the EPICA cores (-798 to -400 kyr BP); E,F The last 22 kyr combined record with a high resolution (interpolated at 100 yr intervals)[21] downloaded as supplementary material from [21]. The EPICA data were downloaded from:

- http://www.ncdc.noaa.gov/paleo/metadata/noaa-icecore-6091.html (CO_2) and
- http://www.ncdc.noaa.gov/paleo/pubs/loulergue2008/loulergue2008.html (CH_4).

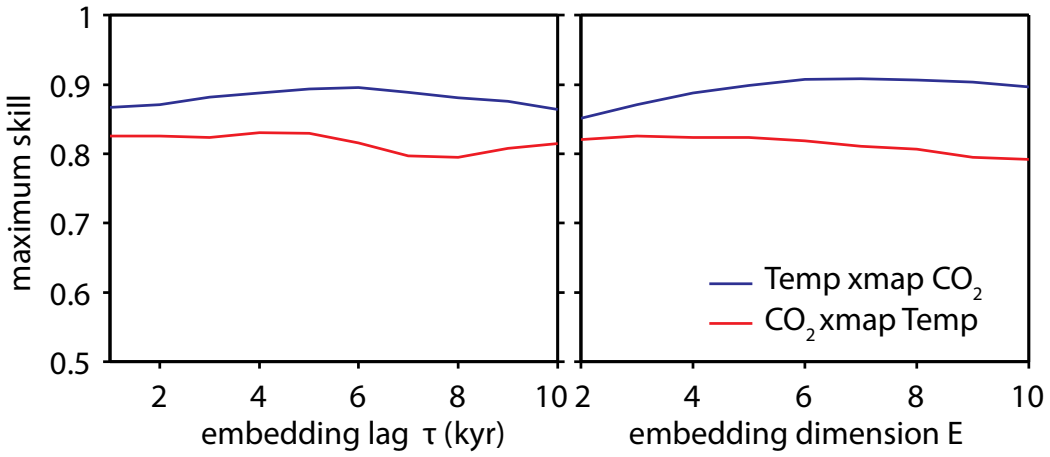

Figure S3.

The sensitivity of maximum CCM skill for the coupling between CO_2 and temperature to the embedding lag τ and the embedding dimension E. This figure shows that the result is robust and insensitive to the choice of these parameters.

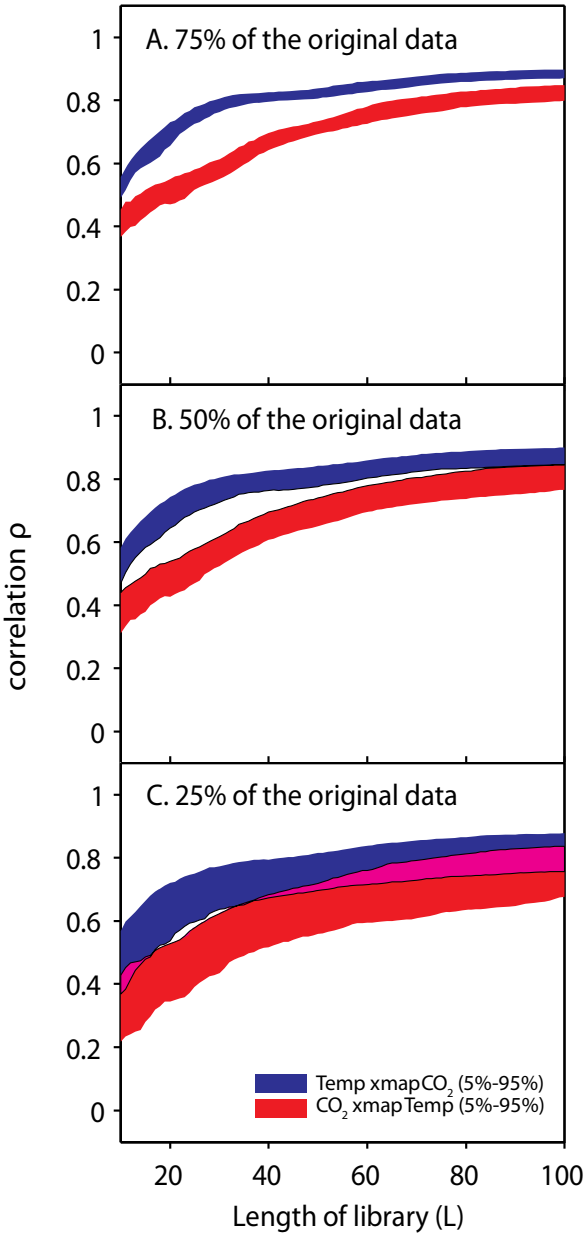

Figure S4.

The sensitivity of CCM results for irregularly spaced data. We removed random portions of the original data of Petit et al.[1] (25%, 50%, and 75%) and linearly interpolated between the remaining points for both temperature and CO_2. This figure shows the 5% and 95% percentiles of CCM skill for 100 randomly generated datasets, and demonstrates the robustness of the method to irregularly spaced data.

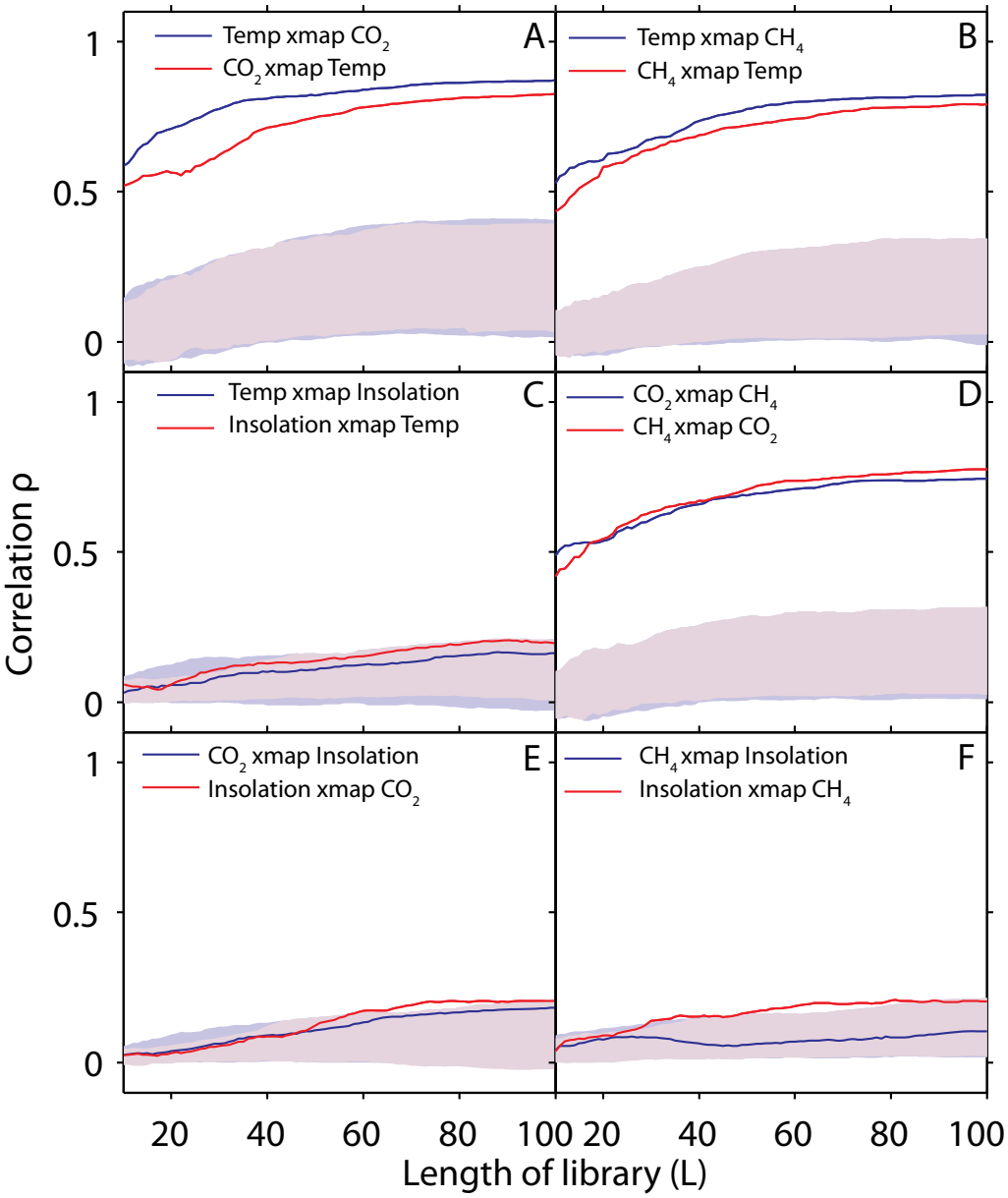

Figure S5.

CCM analyses, as in Figure 2 but with the Ebisuzaki phase shift null model (see Methods). Shaded areas are the 5th to 95th percentiles of CCM skill for 100 surrogate time series from the null model. Results are qualitatively similar to those of Figure 2, where convergence is significant for all pairs except the ones involing insolation.

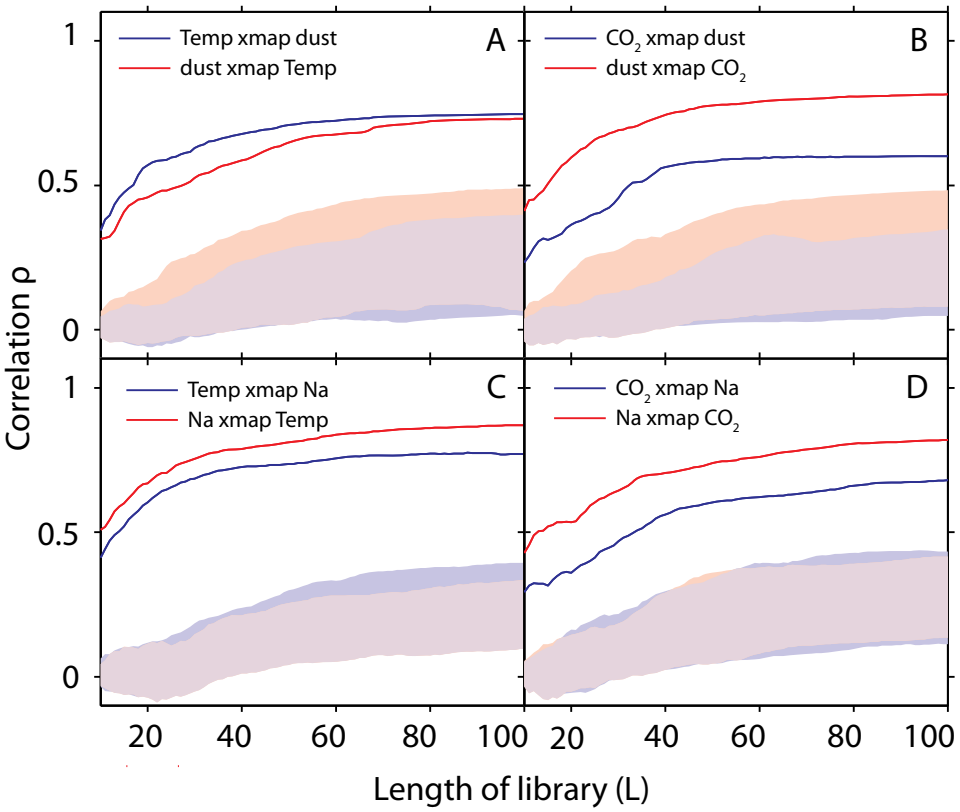

Figure S6.

CCM analyses for sodium (Na) and dust time series. Shaded areas are the 5th to 95th percentiles of CCM skill for 100 surrogate time series from the null model (swap model; see Methods). Results indicate that both sodium (Na) and dust act as proxy variables for the climate system.

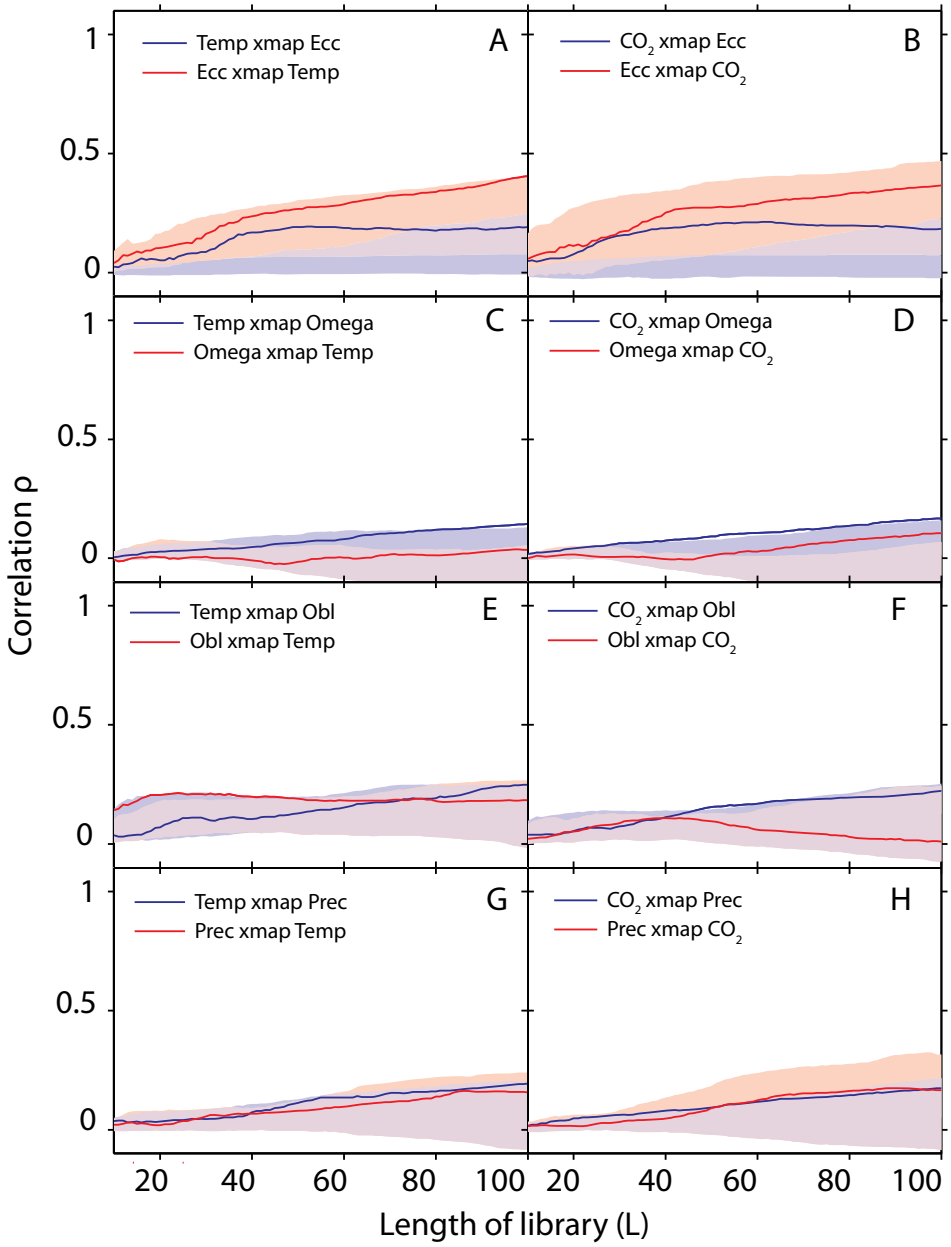

Figure S7.

CCM analyses for different aspects of orbital forcing. Ecc= eccentricity of the earth's orbit, Obl = obliquity or axial tilt, Prec = precession, change in the orientation of the rotational axis, Omega = longitude of perihelion from moving vernal equinox. Shaded areas are the 5th to 95th percentiles of CCM skill for 100 surrogate time series from the null model (swap model; see Methods). Convergence is not significant for any of the variable pairs.

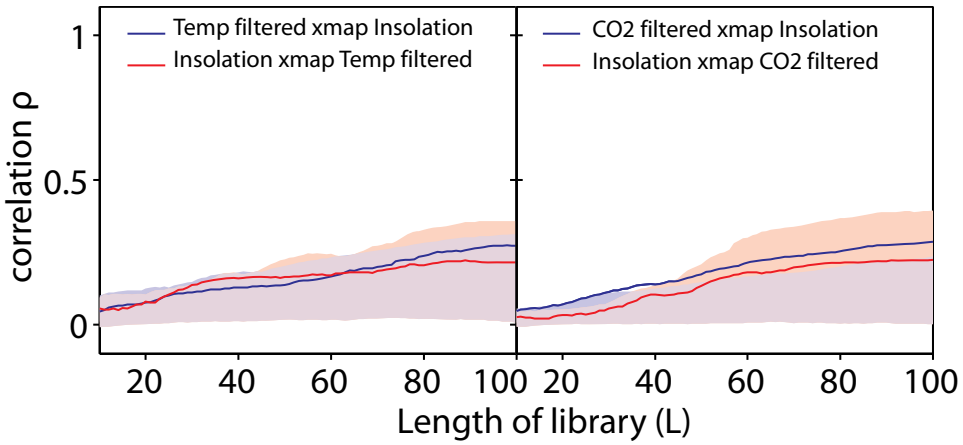

Figure S8.

CCM analyses of temperature and CO_2 time series in which the high frequencies are removed by a Gaussian filter. Shaded areas are the 5th to 95th percentiles of CCM skill for 100 surrogate time series from the null model (swap model). This filtering improved the relation between temperature and insolation somewhat, but it remained not significantly different from the null model.

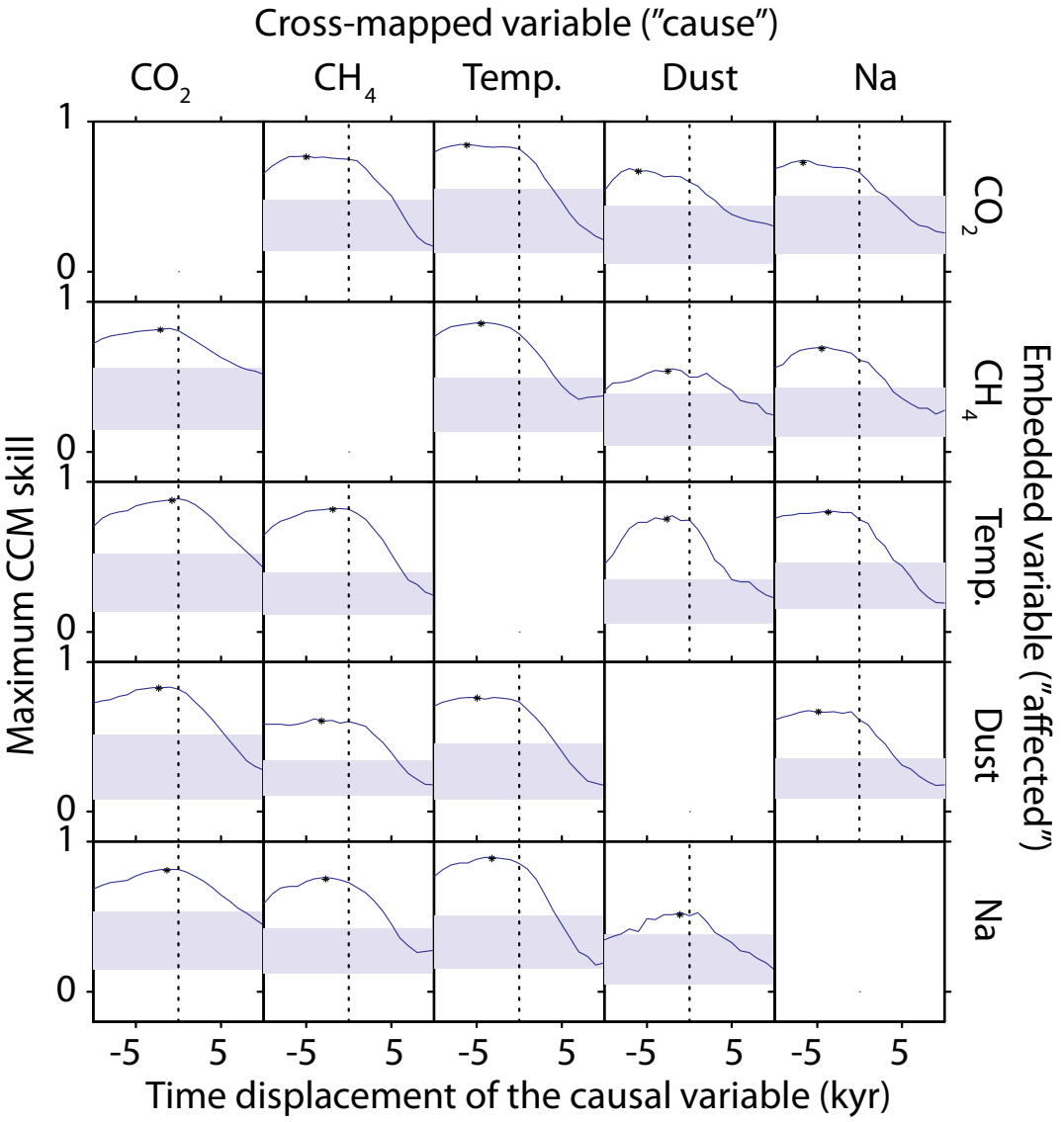

Figure S9.

The effect of lagging the cross-mapped variable on maximum CCM skill. Time displacements are negative if past values of the cross-mapped variable ("cause") are estimated by the embedded variable. Blue shaded areas are the 90% intervals of the null-model (swap model), so CCM skill above this area represents significantly better CCM than the null model. The dashed line is at 0 time displacement, and the optimum displacement is indicated by an asterisk. For the values of the optimal lags see Table S3.

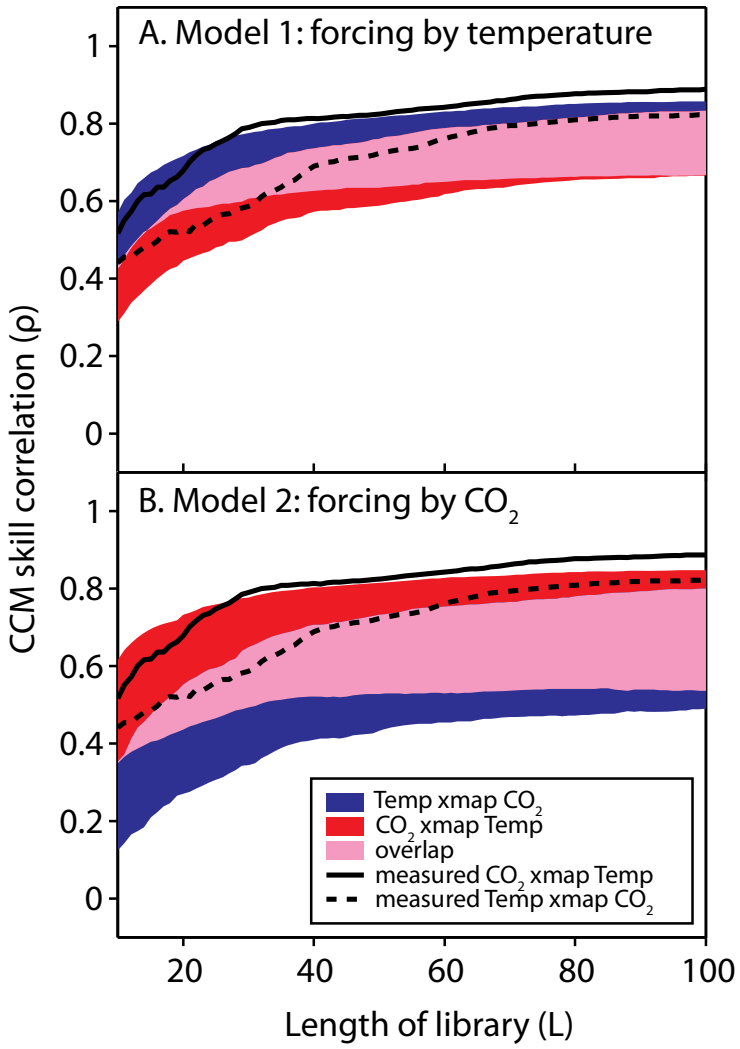

Figure S10.

CCM analyses for 100 runs of the stochastically forced models. We assumed slow dynamics for both CO2 (A: model 1, $r_C = 1$ kyr^{-1}) and temperature (B: model 2, $r_T = 0.5$ kyr^{-1}). The measured skills of the Vostok data are shown in the figure as the solid and dashed black lines.

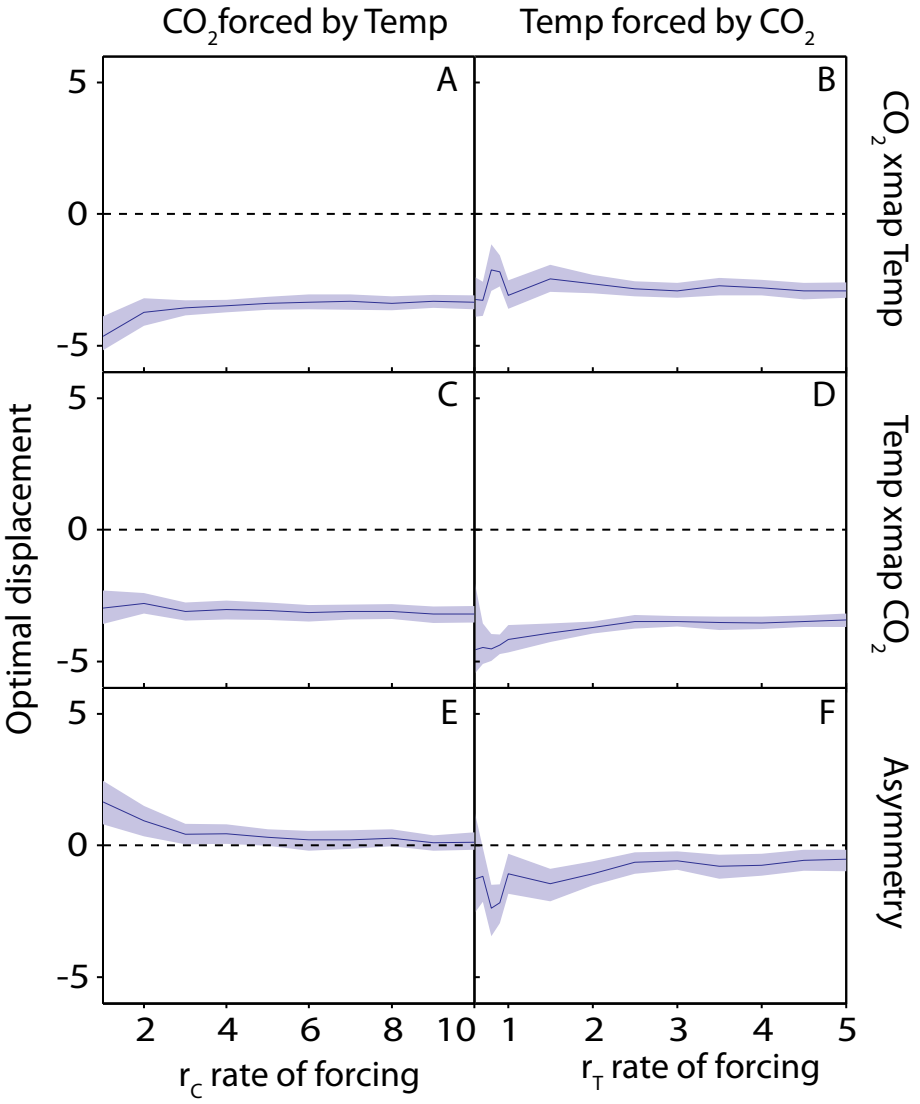

Figure S11.

The optimal time displacement for CCM using data generated by the two unidirectionally-forced models as a function of the speed of the reaction of temperature to CO_2 (left hand panels) and vice versa (right hand panels). Blue area represents the 5%-95% percentiles of 500 bootstrapped library sets and 10 data sets generated with each model; the thick line is the median. Left panels are generated with model 1 (CO_2 is forced by temperature), Right panels with model 2 (Temperature is forced by CO_2). Asymmetry in the response is defined as the difference between the middle and upper graphs.

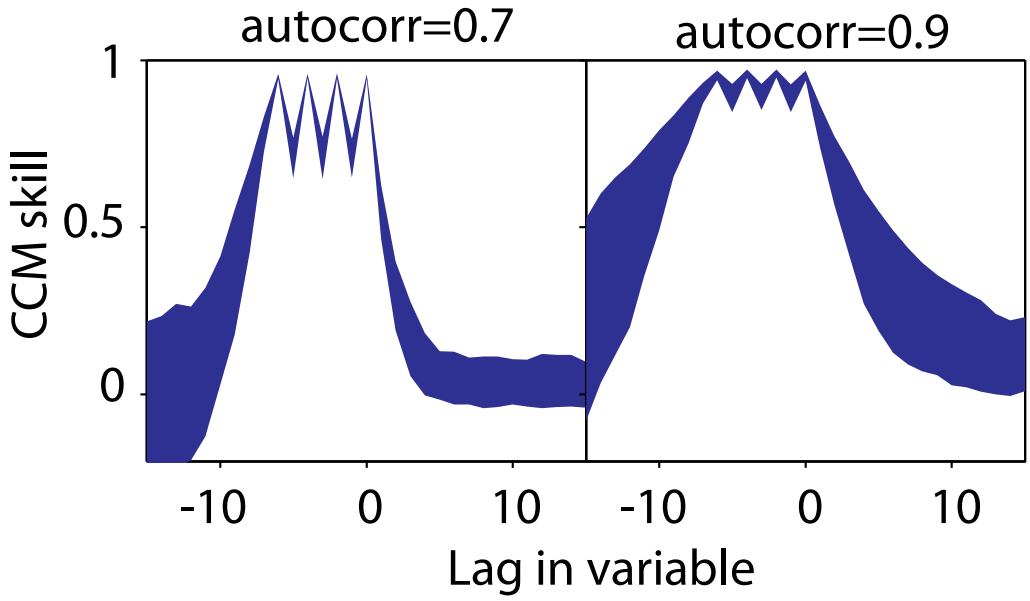

Figure S12.

The optimal lags of CCM of autocorrelated noise when cross-mapped with itself (x xmap x). Blue area represents the 5%-95% percentiles of 100 data sets generated with a simple red noise model. The left panel is generated with an autocorrelation of 0.7, the right hand panel with autocorrelation of 0.9. The highest CCM skill is centred at a lag of -2.5, corresponding to half the length of the fragments in the library used for prediction.

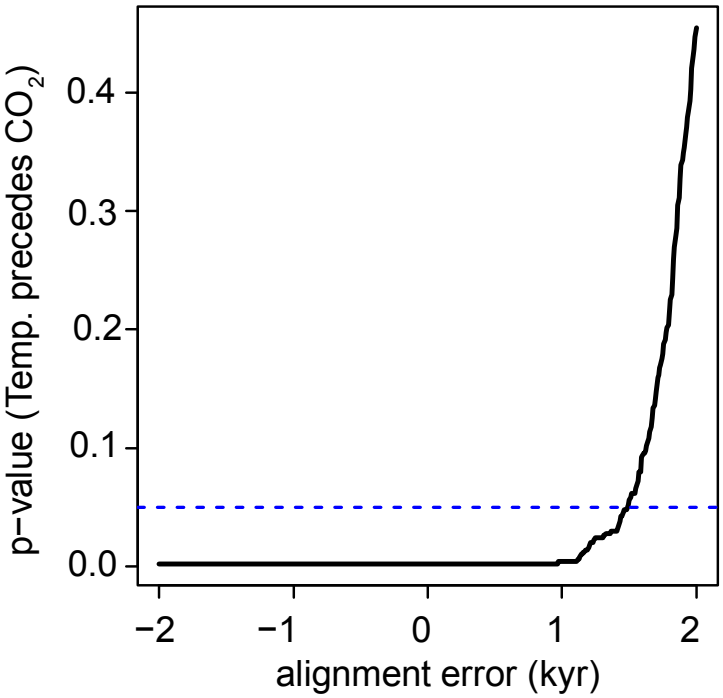

Figure S13.
The effect of a systematic alignment error in the data set on the p-value for a test if the optimal displacement in temperature precedes CO_2. As long as >95% (dashed line) of the bootstrap samples show a positive difference in the optimal lag (i.e. that temperature precedes CO_2), there is significant evidence that temperature has a causal effect on CO_2.

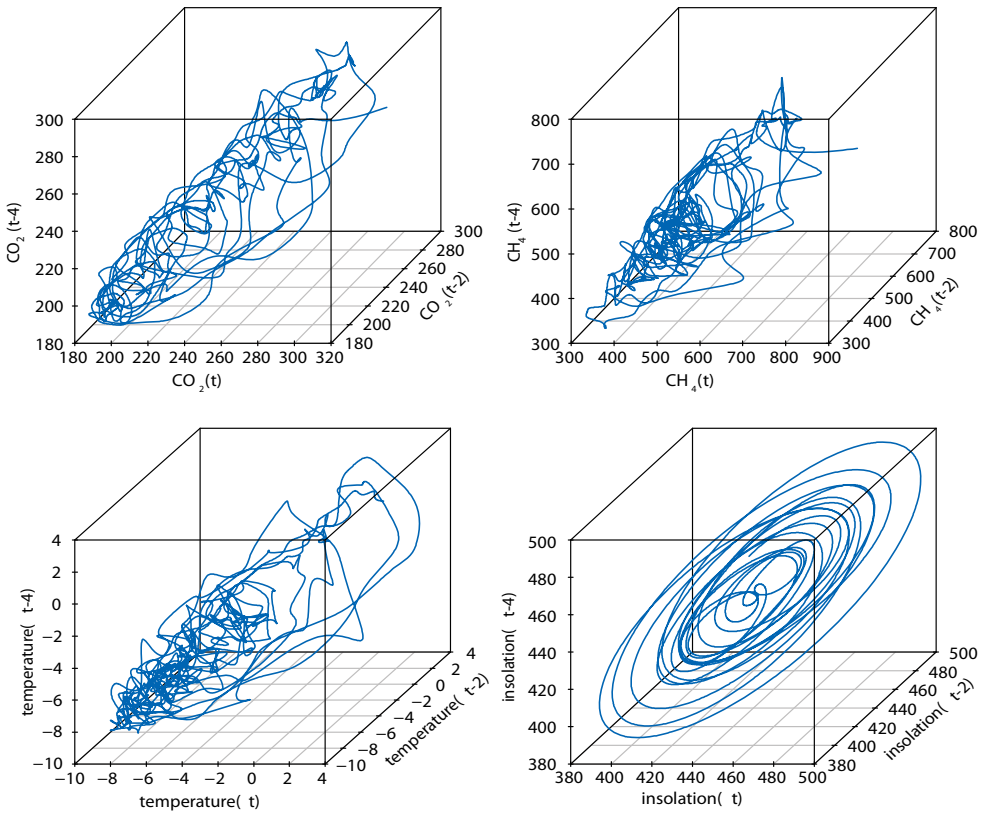

Figure S14.

Three-dimensional Takens delay maps for CO_2, CH_4, temperature, and insolation. Each panel shows the plot of a spline through the lagged-coordinate embedding of each variable (embedding dimension [29] = 3, and the time lag in the coordinates of τ= 2 kyr), giving a depiction of the unfolded attractor for each variable. From visual inspection, we can infer that CO_2, CH_4, and temperature have similar dynamics, and are likely to cross map successfully, whereas insolation appears very different, suggesting that it has different mechanisms and may only weakly influence the other variables.

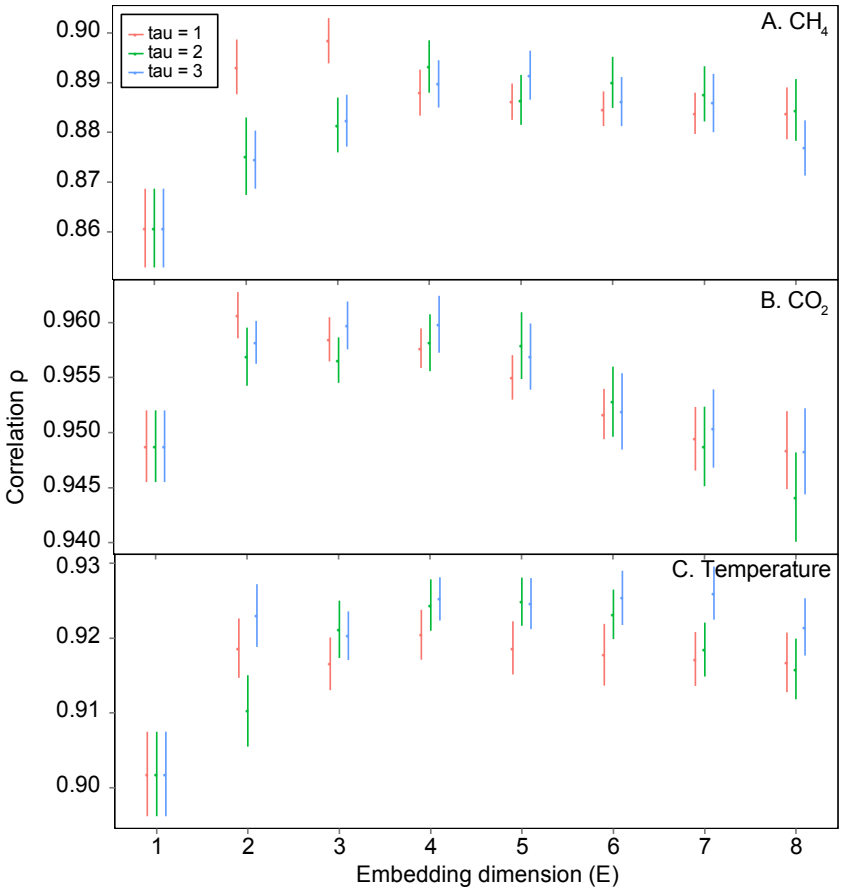

Figure S15. The effect of the embedding dimension E and the time lag τ on prediction skill[29]. The prediction skill was determined by leave-one-out cross-validation of predictability using simplex projection with a library size of 200. The bars show the mean +1 or –1 standard deviation of 100 bootstrapped subsamples.

Supplementary Tables

Table S1.

Convergence of cross mapping of insolation at 65ºN and linearly interpolated CO_2, CH_4, and temperature from the Vostok ice core[1]. For CO_2, CH_4, and temperature we also analyzed a lagged time series shifted +1 and -1 kyr denoted as Temp (-1) and Temp (+1) etc. Results are summarized by fitting the function ($\rho = \rho_{max} - \rho_0 \, e^{-c\,(L-L_0)}$) to the relationship between the library length (L) used for cross mapping and the correlation between predicted and observed. The fit of this function is given by the adjusted R^2.

CCM variables	ρ_0	ρ_{max}	**c**	**adjR^2**	$\rho_{(L=100)}$
Temp *xmap* CO_2	0.338	0.876	0.0582	0.98	0.874
Temp *xmap* CO_2(-1)	0.307	0.878	0.0498	0.989	0.874
Temp *xmap* CO_2(+1)	0.387	0.865	0.061	0.982	0.864
CO_2 *xmap* Temp(-1)	0.363	0.882	0.0264	0.995	0.849
CH_4 *xmap* Temp(-1)	0.334	0.851	0.036	0.989	0.838
CO_2 *xmap* Temp	0.452	0.877	0.0265	0.992	0.836
Temp *xmap* CH_4(-1)	0.351	0.848	0.034	0.99	0.832
Temp *xmap* CH_4	0.394	0.859	0.0291	0.991	0.83
CH_4 *xmap* CO_2(-1)	0.356	0.832	0.0355	0.985	0.818
Temp *xmap* CH_4(+1)	0.446	0.832	0.033	0.992	0.809
CH_4 *xmap* CO_2	0.407	0.812	0.0399	0.989	0.801
CO_2 *xmap* Temp(+1)	0.612	0.853	0.027	0.99	0.8
CH_4 *xmap* Temp	0.399	0.817	0.0335	0.995	0.798
CH_4 *xmap* CO_2(+1)	0.554	0.788	0.0402	0.992	0.773
CO_2 *xmap* CH_4	0.374	0.819	0.0206	0.991	0.76
CH_4 *xmap* Temp(+1)	0.52	0.798	0.0288	0.996	0.759
CO_2 *xmap* CH_4(-1)	0.319	0.774	0.0313	0.993	0.755
CO_2 *xmap* CH_4(+1)	0.46	0.814	0.0222	0.991	0.752
Temp *xmap* Insolation	1.62	1.65	0.00179	0.99	0.269
Insolation *xmap* CO_2	0.473	0.454	0.00977	0.954	0.258
Insolation *xmap* Temp	0.279	0.314	0.014	0.984	0.235
CO_2 *xmap* Insolation	0.303	0.322	0.0133	0.993	0.231
Insolation *xmap* CH_4	0.206	0.248	0.0208	0.982	0.216
CH_4 *xmap* Insolation	0.0724	0.139	0.02	0.813	0.127

Table S2

The same as Table S1 but using spline-interpolated data instead of linearly interpolated data for CH_4, CO_2, and temperature.

CCM variables	ρ_0	ρ_{max}	**c**	**adjR^2**	$\rho_{(L=100)}$
Temp *xmap* CO_2	0.337	0.861	0.0575	0.981	0.859
Temp *xmap* CO_2(-1)	0.303	0.863	0.0492	0.991	0.859
Temp *xmap* CO_2(+1)	0.383	0.855	0.0605	0.985	0.853
CO_2 *xmap* Temp(-1)	0.348	0.867	0.027	0.993	0.836
CO_2 *xmap* Temp	0.433	0.848	0.0276	0.994	0.812
CH_4 *xmap* Temp(-1)	0.303	0.822	0.0353	0.988	0.81
CH_4 *xmap* CO_2(-1)	0.349	0.805	0.0383	0.988	0.794
Temp *xmap* CH_4(-1)	0.338	0.8	0.0335	0.987	0.784
Temp *xmap* CH_4	0.378	0.793	0.0341	0.989	0.776
CH_4 *xmap* CO_2	0.388	0.784	0.0403	0.99	0.773
CO_2 *xmap* Temp(+1)	0.594	0.806	0.0303	0.994	0.767
Temp *xmap* CH_4(+1)	0.413	0.764	0.0358	0.991	0.748
CH_4 *xmap* Temp	0.371	0.748	0.0441	0.995	0.741
CH_4 *xmap* CO_2(+1)	0.557	0.741	0.0422	0.994	0.729
CO_2 *xmap* CH_4(-1)	0.3	0.744	0.0282	0.995	0.721
CO_2 *xmap* CH_4	0.351	0.761	0.0238	0.988	0.72
CH_4 *xmap* Temp(+1)	0.458	0.711	0.0348	0.995	0.691
CO_2 *xmap* CH_4(+1)	0.409	0.724	0.0261	0.989	0.685
Temp *xmap* Insolation	1.11	1.14	0.00266	0.99	0.267
Insolation *xmap* CO_2	0.498	0.487	0.0083	0.952	0.251
CO_2 *xmap* Insolation	0.345	0.358	0.0118	0.993	0.239
Insolation *xmap* Temp	0.277	0.314	0.0141	0.984	0.236
Insolation *xmap* CH_4	0.184	0.214	0.0231	0.986	0.191
CH_4 *xmap* Insolation	0.0598	0.0922	0.135	0.649	0.0922

Table S3

Optimal time displacements for all variable combinations. Columns: cross-mapped variables ("cause") ; Rows: embedded variables ("effect").

	CO_2	CH_4	Temp	dust	Na
CO_2		-4.97	-6.11	-5.99	-6.62
CH_4	-2.12		-4.44	-2.54	-4.44
Temp	-0.74	-1.87		-2.62	-3.68
dust	-2.3	-3.17	-4.89		-4.83
Na	-1.36	-2.7	-3.18	-1.11	